

1 Localized structures in dryland vegetation: Forms and functions

2 Ehud Meron

3 *Department of Solar Energy and Environmental Physics, BIDR, Ben-Gurion University, Sede Boqer*
 4 *Campus, 84990, Israel and Physics Department, Ben-Gurion University, Beer-Sheva, 84105, Israel*

5 Hezi Yizhaq

6 *Department of Solar Energy and Environmental Physics, BIDR, Ben-Gurion University,*
 7 *Sede Boqer Campus, 84990, Israel*

8 Erez Gilad

9 *School of Biological Sciences, Royal Holloway, University of London,*
 10 *Egham, Surrey, TW20 0EX, United Kingdom*

11 (Received 2 March 2007; accepted 9 July 2007)

12 Vegetation patches in drylands are localized structures of biomass and water. We study these
 13 structures using a mathematical modeling approach that captures biomass-water feedbacks.
 14 Biomass-water structures are found to differ in their spatial forms and ecological functions, depend-
 15 ing on species type, soil conditions, precipitation range, and other environmental factors.
 16 Asymptotic spot structures can destabilize to form ring structures, expanding in the radial direction,
 17 or crescent structures, migrating uphill. Stable spot structures can differ in their soil-water distri-
 18 butions, forming water-enriched patches or water-deprived patches. The various biomass-water
 19 structures are expected to function differently in the context of a plant community, forming land-
 20 scapes of varying species diversity. © 2007 American Institute of Physics.

21 [DOI: 10.1063/1.2767246]

22

23 **Vegetation patches surrounded by bare soil are common**
 24 **vegetation forms in dryland landscapes.¹ They form lo-**
 25 **calized structures of biomass and soil-water that vary in**
 26 **size, spatial shape, and function. Vegetation patches can**
 27 **be as small as a few centimeters in diameter (perennial**
 28 **grasses) or as big as a few tens of meters (trees). They can**
 29 **assume spot, ring or crescent shapes, and can deplete the**
 30 **limiting water resource or concentrate it to form habitats**
 31 **for other species. Using a mathematical modeling ap-**
 32 **proach, we study the conditions that give rise to vegeta-**
 33 **tion patches of different shapes, and the roles these**
 34 **patches play in modifying the spatial distribution of the**
 35 **limiting water resource. Among our findings are a cross-**
 36 **over from water-deprived to water-rich patches as the**
 37 **aridity of the system increases, and an instability of spots**
 38 **to rings associated with the root-system size. The results**
 39 **presented here shed new light on the processes of species-**
 40 **diversity change in arid and semiarid regions.**

41

42 I. INTRODUCTION

43 Recent model studies of dryland vegetation^{2–11} support
 44 the view of vegetation pattern formation as a symmetry
 45 breaking phenomenon,¹² induced by water stress. These stud-
 46 ies predict the appearance of five basic vegetation states
 47 along the rainfall gradient: uniform vegetation, gap pattern,
 48 stripe pattern, spot pattern, and bare soil. They also predict
 49 rainfall ranges where two or more different stable vegetation
 50 states coexist. The five basic states along with their multista-
 51 bility ranges provide a wide variety of vegetation patterns,
 52 many of which have been observed in the field.^{13–15} Among

these patterns are sparse vegetation patches surrounded by
 bare soil, which are the subject of this paper. 53 54

Vegetation pattern formation has been attributed to posi-
 tive feedback processes involving plant biomass and
 water.^{6,7,9,11} One process of this kind is associated with in-
 creased infiltration rates at vegetation patches; as the plants
 comprising a vegetation patch grow they often modify the
 local biotic and abiotic environments in ways that increase
 the infiltration rate of surface water into the soil.¹⁶ The in-
 creased infiltration rate at a vegetation patch leads to surface-
 water flow into the patch which increases the soil-water con-
 tent there, and accelerates plant growth. Another positive
 feedback is water uptake by root systems that grow in size in
 response to plant growth. By probing new, unexploited soil
 regions, these root systems increase the amount of soil-water
 available to the plants, thereby accelerating their growth.
 Both processes accelerate plant growth within vegetation
 patches and inhibit it in the surrounding bare soil. 55 56 57 58 59 60 61 62 63 64 65 66 67 68 69 70

The two feedbacks have opposing effects on the water
 balance in vegetation patches; while the infiltration feedback
 acts to concentrate soil-water in a patch, the uptake feedback
 acts to deplete it. Depending on the relative strengths of
 these feedbacks, localized structures that differ in form and
 function are expected to be found. Dominance of the uptake
 feedback is likely to favor species competition and exclu-
 sion, while dominance of the infiltration feedback may favor
 facilitation and coexistence. Surprisingly, despite the exten-
 sive study of vegetation patches in water-limited systems,
 and the interactions among the plant species comprising
 them, very little is known about the soil-water distributions
 in these patches.¹⁷ 71 72 73 74 75 76 77 78 79 80 81 82 83

TABLE I. Relations between the nondimensional variables and parameters appearing in Eqs. (1)–(4) and their dimensional counterparts. The quantities B and W are the dimensional biomass and soil-water densities in units of (kg/m²), H is the dimensional height of the water layer above ground level in units of mm, and all other dimensional quantities are defined in Table II.

Quantity	Scaling	Quantity	Scaling
b	B/K	p	$\Delta P/MN$
w	$\Delta W/N$	δ_b	D_B/MS_0^2
h	$\Delta H/N$	δ_w	D_W/MS_0^2
q	Q/K	δ_h	$D_H N/M \Delta S_0^2$
ν	N/M	ζ	$\Delta Z/N$
α	A/M	ρ	R
η	EK	t	MT
γ	$\Gamma K/M$	\mathbf{x}	\mathbf{X}/S_0

TABLE II. Definitions of dimensional model quantities and their units.

Parameter	Units	Description
K	kg/m ²	Maximum standing biomass
Q	kg/m ²	Biomass reference value beyond which infiltration rate under a patch approaches its maximum
M	yr ⁻¹	Rate of biomass loss due to mortality and disturbances
A	yr ⁻¹	Infiltration rate in fully vegetated soil
N	yr ⁻¹	Soil-water evaporation rate
E	(kg/m ²) ⁻¹	Relative root's extension per unit biomass density
Λ	(kg/m ²) ⁻¹ yr ⁻¹	Biomass growth rate per unit soil-water density
Γ	(kg/m ²) ⁻¹ yr ⁻¹	Soil-water consumption rate per unit biomass density
D_B	m ² /yr	Seed dispersal coefficient
D_W	m ² /yr	Transport coefficient for soil water
D_H	m ² /yr (kg/m ²) ⁻¹	Bottom friction coefficient between surface water and ground surface
S_0	m	Minimal root length
$Z(\mathbf{X})$	mm	Topography function
P	kg/m ² yr ⁻¹	Precipitation rate
R	...	Evaporation reduction due to shading
f	...	Infiltration contrast between bare soil and vegetated soil

84 In this paper we use a mathematical modeling approach
 85 to study biomass and soil-water distributions associated with
 86 vegetation patches of a single plant species. We study the
 87 relative strength of the infiltration and uptake feedbacks at
 88 various environmental conditions and discuss the implica-
 89 tions of the resulting water-biomass distributions on ecosys-
 90 tem engineering, species diversity, and desertification. This is
 91 a synthetic review of earlier results,^{9–11,18} complemented by
 92 new results related to patch-form instabilities.

93 **II. A DYNAMIC MODEL FOR WATER-LIMITED**
 94 **VEGETATION**

95 In earlier studies^{9,11} we developed model equations to
 96 describe vegetation dynamics in water-limited systems. The
 97 model equations in nondimensional form are

98
$$b_t = G_b b(1 - b) - b + \delta_b \nabla^2 b,$$

99
$$w_t = \mathcal{I}h - \nu(1 - \rho b)w - G_w w + \delta_w \nabla^2 w, \quad (1)$$

100
$$h_t = p - \mathcal{I}h + \delta_h \nabla^2 h^2 + 2\delta_h \nabla h \cdot \nabla \zeta + 2\delta_h h \nabla^2 \zeta,$$

face water into the soil in vegetation patches. The feedback
 is captured by several terms in the model equations: (a) the
 term $\mathcal{I}h$ in the equation for w , where the infiltration rate \mathcal{I} is
 given by²⁰

$$\mathcal{I}(\mathbf{x}, t) = \alpha \frac{b(\mathbf{x}, t) + qf}{b(\mathbf{x}, t) + q}, \quad (2)$$

(b) the water-dependent biomass growth rate, G_b [see Eq. (3)], and (c) the water flow terms in the equation for h , parameterized by the nondimensional friction coefficient δ_h . A typical form of \mathcal{I} is shown in Fig. 1. For $f < 1$, the infiltration rate increases monotonically with the biomass density. As a result, higher biomass densities imply higher soil-water densities and therefore higher biomass-growth rates. The strength of this feedback can be controlled by the parameter f . Lower values of f , modeling, e.g., the existence of

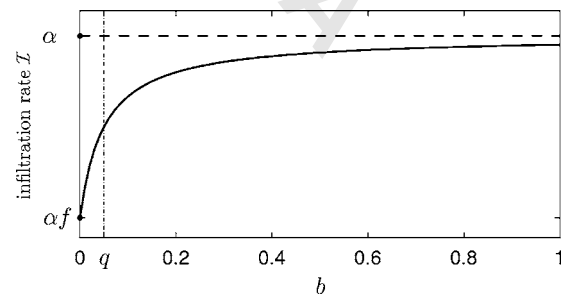


FIG. 1. The infiltration rate \mathcal{I} as a function of biomass density b . The infiltration contrast between bare and vegetated soil is quantified by the parameter f , where $0 < f < 1$; when $f = 1$ the contrast is zero and when $f = 0$ the contrast is maximal. Note the weak dependence of the infiltration rate on biomass for $b \gg q$. Reprinted from Ref. 11. Copyright (2007), with permission from Elsevier.

101 where $b(\mathbf{x}, t)$ represents the areal density of overground veg-
 102 etation biomass, $w(\mathbf{x}, t)$ represents the areal soil-water den-
 103 sity, and $h(\mathbf{x}, t)$ is the height of a thin water layer above the
 104 ground level described by a prescribed topography function
 105 $\zeta(\mathbf{x})$ [where $\mathbf{x} = (x, y)$]. The relations between the nondimen-
 106 sional quantities appearing in (1) and their dimensional
 107 counterparts are given in Table I. The definitions of the latter
 108 and their units are given in Table II. Noteworthy is the non-
 109 dimensional precipitation parameter p , which shows the
 110 equivalence of increasing the precipitation rate P and de-
 111 creasing the biomass-loss rate M . Depending on the plant
 112 life-form to be considered we will assume constant or time-
 113 periodic forms for the precipitation parameter, representing
 114 mean annual rainfall rate or seasonal rainfall variations.
 115 The model captures various feedback processes involv-
 116 ing biomass growth, root augmentation, water uptake, and
 117 water evaporation, as described below.¹⁹ The relative
 118 strengths of these processes determine the forms and func-
 119 tions of localized vegetation patches.
 120 *Infiltration feedback.* This is a positive feedback between
 121 biomass and water due to increased infiltration rates of sur-

136 biogenic crusts,²¹ correspond to lower infiltration rates in
 137 bare soil relative to the infiltration rates in vegetation
 138 patches. This infiltration contrast increases the surface water
 139 flow towards the vegetation patches, and thereby strengthens
 140 the infiltration feedback.

141 *Root-augmentation feedback.* This is a positive feedback
 142 between the overground biomass and the underground roots.
 143 As the plant grows its root system extends in size and probes
 144 new soil regions where water can be taken up. As a result the
 145 amount of water available to the plant increases and the plant
 146 grows even further. This feedback is captured by the nonlin-
 147 ear and nonlocal form of the biomass growth rate

$$G_b(\mathbf{x}, t) = \nu \int_{\Omega} g(\mathbf{x}, \mathbf{x}', t) w(\mathbf{x}', t) d\mathbf{x}', \quad (3)$$

$$g(\mathbf{x}, \mathbf{x}', t) = \frac{1}{2\pi} \exp\left[-\frac{|\mathbf{x} - \mathbf{x}'|^2}{2(1 + \eta b(\mathbf{x}, t))^2}\right],$$

151 where the integration is over the entire physical domain Ω .
 152 The Gaussian kernel g represents the root system whose size
 153 (width of the Gaussian) grows as the biomass density b
 154 grows. The strength of this feedback is quantified by the
 155 parameter η ; the larger η the stronger the feedback. Larger η
 156 values represent species that allocate more resources to root
 157 growth.

158 *Uptake feedback.* This is a negative feedback between
 159 biomass and water due to water-uptake by the plant's roots.
 160 The depletion of soil-water at any given point is due to all
 161 plants whose roots extend to this point. The feedback is cap-
 162 tured by the term $-G_w w$ in the equation for w , where the
 163 water consumption rate, G_w , increases with the biomass den-
 164 sity according to

$$G_w(\mathbf{x}, t) = \gamma \int_{\Omega} g(\mathbf{x}', \mathbf{x}, t) b(\mathbf{x}', t) d\mathbf{x}'. \quad (4)$$

166 *Shading feedback:* This is a positive feedback between
 167 biomass and soil-water due to reduced evaporation at vegeta-
 168 tion patches. The feedback is captured by the biomass depen-
 169 dence of the evaporation term, $-\nu(1 - \rho b)w$, in the equation
 170 for w . Unlike the infiltration feedback, the increase of soil-
 171 water content under a vegetation patch does not involve the
 172 depletion of soil-water from the surroundings of the patch.

173 III. EXTENDED VEGETATION STATES

174 We consider in this section solutions of Eqs. (1)–(4) for
 175 constant values of the precipitation parameter p , representing
 176 mean annual rainfall rates. This approximation is valid for
 177 species such as woody plants whose growth-time scales are
 178 much longer than a year. The simplest solutions describe a
 179 stationary uniform bare-soil state and a stationary uniform-
 180 vegetation state, denoted in Fig. 2 by \mathcal{B} and \mathcal{V} , respectively.

181 The bare soil solution is given by $b=0$, $w=p/\nu$, and h
 182 $=p/\alpha f$. It is linearly stable for $p < p_c = 1$ and it loses stability
 183 at $p = 1$ to uniform perturbations.^{11,22} The uniform vegetation
 184 solution, \mathcal{V} , exists for $p > p_c = 1$ in the case of a supercritical
 185 bifurcation and for $p > p_1$ (where $p_1 < 1$) in the case of a

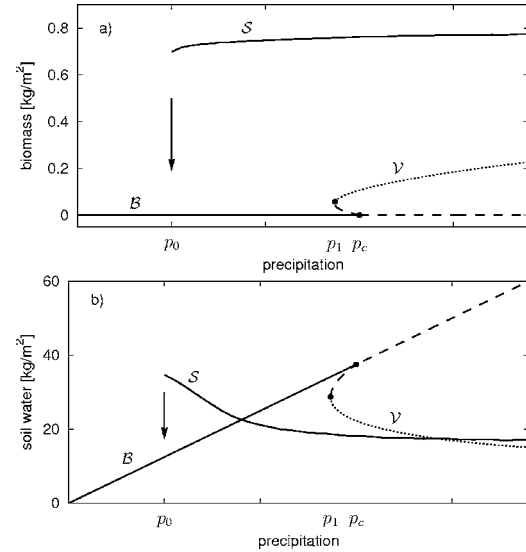


FIG. 2. Solution branches for the biomass and soil-water densities along the low end of the precipitation axis. The branches \mathcal{B} and \mathcal{V} denote, respectively, bare-soil and uniform-vegetation solutions. The branch \mathcal{S} denotes a spot-pattern solution. In panel (a) it denotes the amplitude of the biomass density, while in panel (b) it denotes the soil-water density at the center of a biomass spot. The figure shows the coexistence range, $p_0 < p < p_c$, of stable spot-pattern and bare-soil solutions, and illustrates the occurrence of a catastrophic shift (see arrow) as the precipitation drops below p_0 . The \mathcal{S} branch was calculated by numerical integration of the model equations [Eqs. (1)–(4)]. Parameters: $f=0.1$, $\nu=\delta_w=3.333$, $\alpha=33.333$, $q=0.05$, $\delta_h=333.333$, $\eta_1=3.5$, $\gamma_1=16.667$, $\rho_1=0.95$, and $\delta_b=0.033$.

subcritical bifurcation. It is stable, however, only beyond another threshold, $p=p_2 > p_1$ (outside the range shown in Fig. 2).

As p is decreased below p_2 the uniform vegetation solution, \mathcal{V} , loses stability to nonuniform perturbations in a finite wave number (Turing-type) instability. These perturbations grow to form extended pattern states. The following sequence of basic pattern states has been found at decreasing precipitation values for plane topography:^{9,11} hexagonal gap patterns, stripe patterns, and hexagonal spot patterns. The \mathcal{S} branch in Fig. 2 shows the amplitude of the spot-pattern solution. Note the bistability range, $p_0 < p < p_c$, of bare-soil (\mathcal{B}) and spot-pattern (\mathcal{S}) solutions. Bistability ranges exist for any other consecutive pair of states along the precipitation axis: spots and stripes, stripes and gaps, and gaps and uniform vegetation.

IV. LOCALIZED BIOMASS-WATER STRUCTURES

Localized structures often appear in bistability ranges of extended states.²³ Here we focus on the range $p_0 < p < p_c$, where spot patterns and bare soil are both stable solutions of Eqs. (1)–(4). We take the precipitation parameter p to be a constant representing the mean annual rainfall rate. This restricts our consideration to plant species (e.g., woody) whose growth time scales are long in comparison to the seasonal time scale.

In the bistability range, $p_0 < p < p_c$, we numerically find localized spot solutions representing isolated spot-like vegetation patches in an otherwise bare-soil area. A solution representing such patches is shown in Figs. 3(b) and 3(c). Fig-

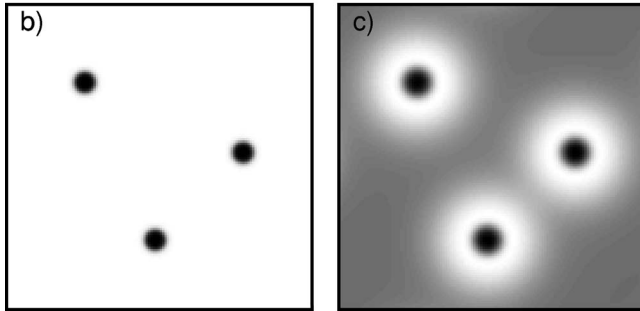


FIG. 3. Spot-like vegetation patches in the field (a) and as obtained by numerically solving Eqs. (1)–(4) (b), (c). Shown in (a) are patches of *Urginea maritima* observed in the Negev desert (80 mm/yr). (Photography by E. Meron.) Patch sizes are of the order of 40 cm. The spot solutions in (b) and (c) describe localized structures of biomass and soil water, respectively. Dark shades of gray represent high biomass or soil-water densities. Parameters (b), (c): $P=75$ mm/yr and all other parameters are as in Fig. 2. Domain sizes in (b), (c) are 7.5×7.5 m².

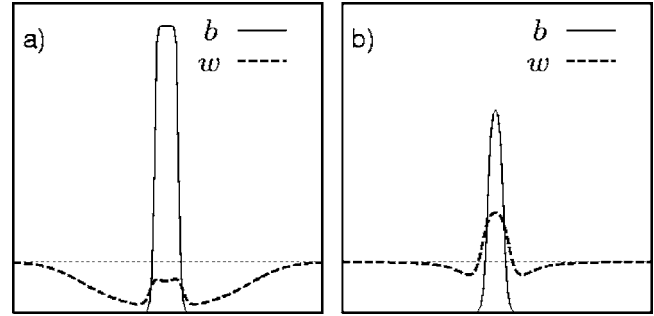


FIG. 4. Spatial profiles of the variables b and w as affected by the parameter that controls the root-augmentation feedback, η . The profiles are cross sections of two-dimensional spot solutions of the model Eqs. (1)–(4). The horizontal dotted lines denote the soil-water density at bare soil. A strong root-augmentation feedback ($\eta=5.5$) results in soil-water depletion (a). A weak root-augmentation feedback ($\eta=2$), and sufficiently strong infiltration feedback, leads to soil-water concentration (b). The domain size is 5 m. Values of all other parameters are as in Fig. 2 with $p=0.5$ (75 mm/yr).

[Fig. 4(b)], and the solution represents a water-enriched patch. 240
241

Water-enriched patches are obtained for small- η species (compact root systems) and small f values, representing strong infiltration contrasts between bare soil and vegetation patches (e.g., $f=0.1$ in Fig. 4). Such a situation is often realized in nature when the bare soil is covered by a biological crust.²¹ What would be the effect of a disturbance that increases f , e.g., by removing the fragile crust? As Fig. 5 demonstrates, the general effect, at least for sufficiently high f 242
243
244
245
246
247
248
249

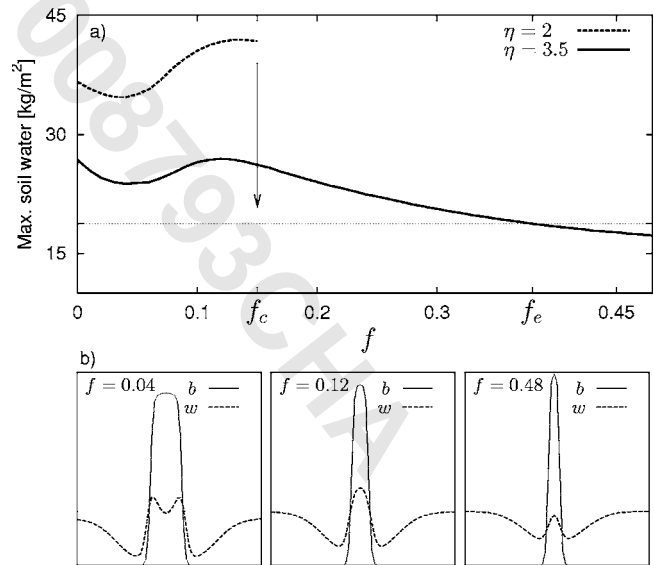


FIG. 5. Model calculations showing the effects of soil disturbances on spot-like vegetation patches. (a) The maximal soil-water density under a patch at increasing values of f (modeling e.g., gradual crust removal) for species characterized by $\eta=2$ (dashed line) and $\eta=3.5$ (solid line). The lower- η species concentrates more water but is not resilient to strong disturbances ($f > f_c$). The higher- η species is resilient to strong disturbances but loses the capability to concentrate soil-water when the disturbance is too strong ($f > f_e$). (b) Spatial profiles of b and w at increasing f values. In the small f range a ring-shape water distribution ($f=0.04$) changes into a spot-shape distribution ($f=0.12$). Parameters are as in Fig. 2 with $p=0.5$ (75 mm/yr). Reprinted [panel (a)] from Ref. 11. Copyright (2007), with permission from Elsevier.

215 ure 3(a) shows a patch of *Urginea maritima* observed in the
216 Negev desert. The stability of a localized spot structure stems
217 from the depletion of the water resource in the immediate
218 vicinity of the spot [see Fig. 3(c)] which prevents its further
219 expansion. Contributing to this depletion process are the in-
220 filtration, root-augmentation, and uptake feedbacks. These
221 feedbacks, together with the shading feedback, also deter-
222 mine the water balance within the spot, or under the vegeta-
223 tion patch it represents. In the following we study how this
224 water balance is affected by species traits and by environ-
225 mental changes.

226 Of the four feedbacks, the infiltration and shading feed-
227 backs act to increase the soil-water content in a spot, whereas
228 the uptake and root-augmentation feedbacks act to decrease
229 it. Figure 4 shows the biomass and soil-water distributions in
230 and around localized spot structures of species characterized
231 by different values of the parameter η , which controls the
232 strength of the root-augmentation feedback. When the root-
233 augmentation feedback is strong (large η) the soil-water den-
234 sity in the spot and its vicinity is lower than in bare soil [Fig.
235 4(a)]. This solution represents a water-deprived patch, result-
236 ing from the high water-uptake by the large root systems in
237 the patch. The water balance is inverted when the root-
238 augmentation feedback is sufficiently weak (small η); the
239 soil-water density in the spot area is larger than in bare soil

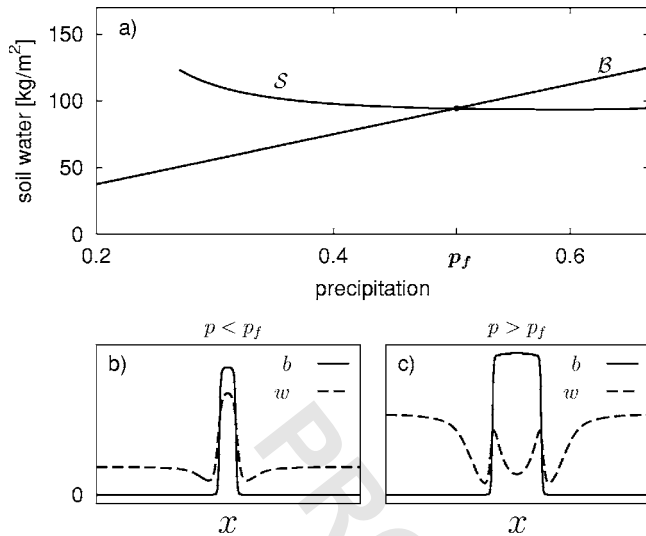


FIG. 6. A transition from water-deprived to water-enriched patches as a result of a precipitation down shift. The lines B and S in panel (a) show, respectively, the soil-water density in bare soil and the maximal soil-water density in a spot structure as functions of the precipitation rate p . Above (below) a crossover point, $p = p_f$, the water content in a spot structure is lower (higher) than in bare soil. Panels (b) and (c) show spatial profiles of b and w at precipitation rates below (187.5 mm/yr) and above (480 mm/yr) the crossover point $p_f = 0.504$ which corresponds to 378 mm/yr. Parameters: $\nu = \delta_w = 1.667$, $\alpha = 16.667$, $q = 0.05$, $f = 0.1$, $\delta_h = 416.667$, $\eta = 3.5$, $\gamma = 2.083$, $\rho = 0.95$, $\delta_b = 0.0167$.

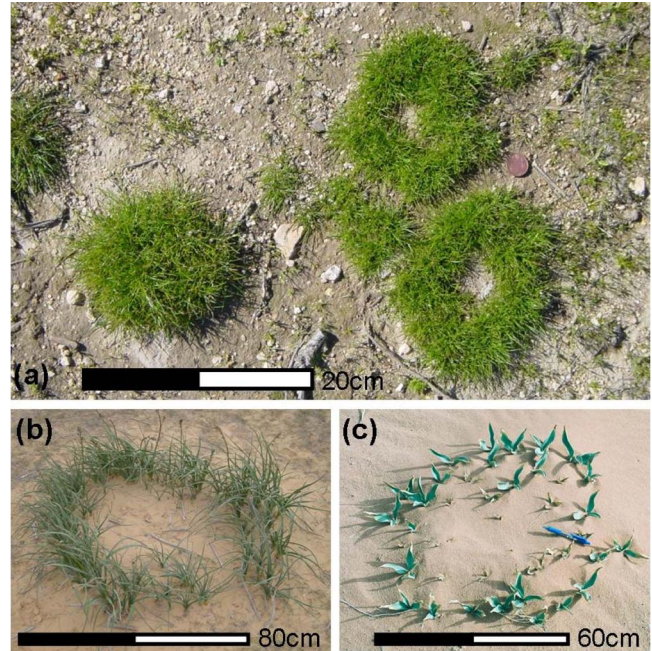


FIG. 7. Ring patterns in nature. (a) Mixture of rings and spots of *Poa bulbosa* observed in the Northern Negev (250 mm/yr). (b) A ring of *Asphodelus ramosus* observed in the Negev desert (170 mm/yr). (c) A ring of *Urginea maritima* observed in Wadi Rum, Jordan (50 mm/yr). Photography by J. von Hardenberg (a) and H. Yizhaq (b), (c). Reprinted from Ref. 18.

AQ:
#5

250 values, is reduced soil-water content in the patch area be-
 251 cause of increased infiltration in the surrounding bare soil.
 252 The strength of the root-augmentation feedback, however, is
 253 of critical importance. If this feedback is not strong enough
 254 (i.e. η large enough) a critical value, $f = f_c$, exists, beyond
 255 which the localized structure collapses to zero [down arrow
 256 in Fig. 5(a)]. A tradeoff therefore exists between the capabil-
 257 ity of a vegetation patch to concentrate the water resource
 258 and its resilience to disturbances.

259 Another possible consequence of increasing f from very
 260 low values is a change in the soil-water distribution in the
 261 patch area from a ringlike shape, where the highest density is
 262 at the patch periphery, to a spot-like shape, where the highest
 263 density is at the center of the patch. Such a change is seen in
 264 the small f range of Fig. 5(b). The mechanism of this change
 265 is related to the area occupied by the biomass spot (vegeta-
 266 tion patch) which decreases as f increases. Bigger patches
 267 contain more individuals that compete for the water resource.
 268 The competition is strongest at the patch center and therefore
 269 acts to deplete the soil-water content there more than in other
 270 points of the patch. In addition, surface water flowing from
 271 the patch surrounding infiltrate mostly at the patch periphery,
 272 thereby increasing the soil-water content there as compared
 273 with the patch center.

274 A different type of environmental change, that may af-
 275 fect the water balance within a spot structure, is a precipita-
 276 tion downshift, such as a prolonged drought. As Fig. 6 dem-
 277 onstrates, at high precipitation rates ($p > p_f$) the soil-water
 278 density in the spot and its vicinity is lower than in bare soil,
 279 while at low precipitation rates ($p < p_f$) the soil-water den-
 280 sity in the spot is higher than in bare soil. The mechanism of
 281 this crossover from water-deprived to water-enriched patches

as a result of a precipitation downshift is again related to the
 patch size. At lower precipitation rates the patches are
 smaller, thus having fewer water-consuming plant individ-
 uals in any area element of the patch. The infiltration rate, on
 the other hand, is hardly reduced because of the weak depen-
 dence of the infiltration rate on biomass for grown-up plants
 (see Fig. 1).

Changes in patch structures, from water-deprived to
 water-enriched patches, or from ring-shape to spot-shape wa-
 ter distributions, have important implications for interspecific
 plant interactions and species diversity changes, as discussed
 in Sec. VI.

V. INSTABILITY TO RING AND CRESCENT STRUCTURES

Another common patch form observed in nature is the
 ring.²⁴⁻²⁶ Figure 7 shows examples of ring-shape patches
 formed by different plant species in water-limited systems.
 Under what conditions do ringlike patches appear and how
 are these structures related to spot-like patches? In this sec-
 tion we use the model Eqs. (1)–(4) to study ring and
 crescent-like patch forms. Since rings have been observed
 with species spanning a wide range of growth rates, includ-
 ing fast growing herbaceous species, we study these ques-
 tions using the model Eqs. (1)–(4) with time-periodic pre-
 cipitation rates, $p(t)$, representing seasonal rainfall
 variations. Specifically, a square-wave form, representing a
 four-month rainy period followed by an eight-month dry pe-
 riod, is chosen for $p(t)$.

To quantify the difference between spots and rings we
 introduce “ring index”¹⁸ defined as

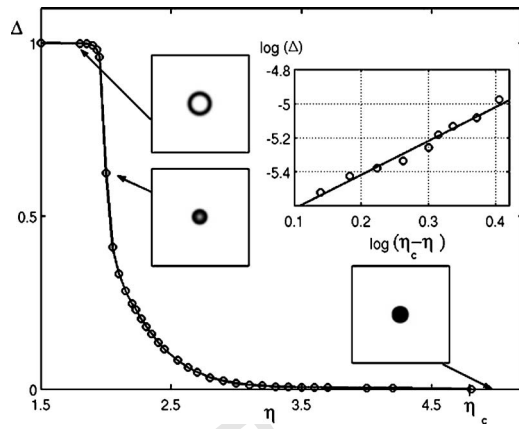


FIG. 8. Model calculations showing a transition from spots to rings as the lateral augmentation of the roots per unit biomass growth, η , decreases. The small insets show typical patch forms (at dimensional time $t=50$ years): spots at large η , latent rings at intermediate η , and visible rings at small η . The spots and latent rings are asymptotic forms while visible rings keep expanding. The larger inset shows a log-log plot supporting the scaling relation $\Delta \sim (\eta_c - \eta)^2$, where $\eta_c = 4.8$. Parameters: $p=0.88$ (220 mm/yr), $\nu = 4$, $\alpha=160$, $q=0.05$, $\rho=1$, $\gamma=5$, $f=0.1$, $\delta_b=0.02$, $\delta_w=2$, $\delta_i=200$. Reprinted from Ref. 18.

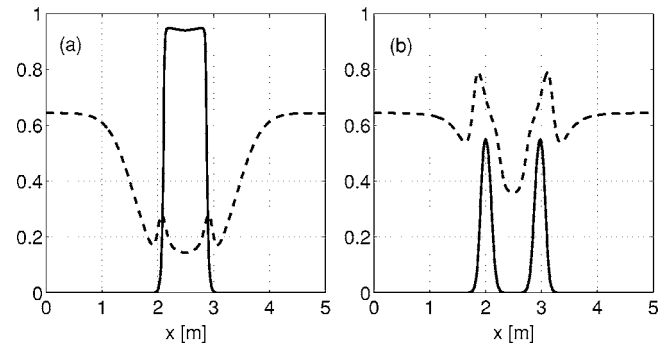


FIG. 9. Transsects of two-dimensional spatial distributions of biomass and soil-water density for (a) a stationary spot solution ($\eta=3.2$), and (b) an expanding ring solution ($\eta=1.6$). Dimensional time is $t=50$ years and all other parameters are as in Fig. 8.

having a lower uptake rate, can keep expanding. The increased water stress at the spot's core will eventually lead to a central die-back and ring formation. Figure 9 shows biomass and soil-water profiles supporting this mechanism; the soil-water density at the forefront of a spot (ring) is significantly lower (higher) than the soil-water density in bare soil. Latent rings, like spots and unlike visible rings, approach asymptotic forms characterized by fixed averaged radii.

The results also suggest that ring-forming species all have compact root systems in the lateral directions. This appears consistent with the observation that all plant species showing ring formation expand vegetatively following "phalanx-growth" strategy.²⁷ In this strategy new individuals are added at the boundary of the biomass patch and are connected to the clone by very short stems. This spatial expansion strategy results in highly dense patches of individuals whose roots are laterally confined.

For a given ring-forming species, characterized by some η value smaller than η_c , decreasing the mean annual precipitation rate \bar{p} , should result in the formation of a stable spot structure. This is because the soil-water density in the neighborhood of a small growing spot can drop below the level

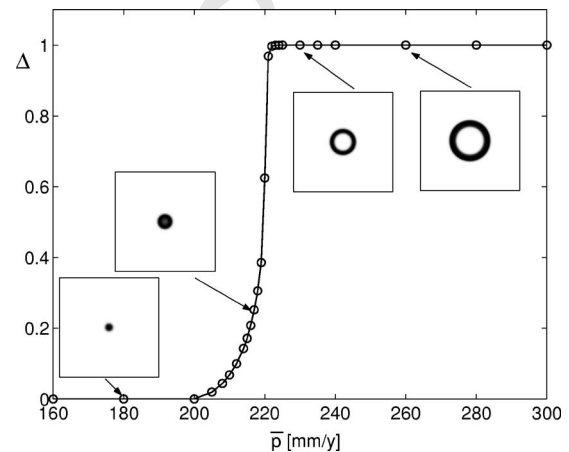


FIG. 10. Model calculations showing a transition from spots to rings as the mean annual precipitation rate, \bar{p} , increases. The insets show typical patch forms (at dimensional time $t=50$ years): spots at low \bar{p} , latent rings at intermediate \bar{p} , and visible rings at high \bar{p} . Parameters: $\eta=2$ and all other parameters are as in Fig. 8.

$$\Delta = \frac{b_{\max} - b_{\text{core}}}{b_{\max}}, \quad (5)$$

where b_{\max} stands for the maximal biomass density in the patch and b_{core} for the biomass density in the patch center. The value $\Delta=0$ corresponds to a spot-like patch, where the maximal biomass density occurs at the core of the patch, $\Delta=1$ corresponds to a visible biomass ring ($b_{\text{core}}=0$), and intermediate values, $0 < \Delta < 1$, represent latent rings.

Since spot structures appear to be stabilized by depletion of soil-water in the spot's surroundings, we chose to vary the parameter η which controls the root-system size and thus the water uptake in the vicinity of the spot. Figure 8 shows a graph of the ring index Δ as a function of η . At large η values the ring index vanishes, indicating the prevalence of stable spots. At small η values the ring index approaches unity, indicating the prevalence of visible rings. In between there is an η range of latent rings.

To better quantify the behavior near the transition point, $\eta = \eta_c$, from spots to latent rings we consider the core region where the biomass density can be expanded as $b(r) = b_{\text{core}} + a_2(\eta_c - \eta)r^2 - a_4r^4 + \dots$. Here, r is the radial coordinate and a_2, a_4 are constants. A simple calculation shows that the ring index scales with the distance, $\eta_c - \eta$, from the transition point like $\Delta \sim (\eta_c - \eta)^2$, whereas the ring radius scales like $R \sim (\eta_c - \eta)^{1/2}$. The log-log plot inset in Fig. 8 supports these scaling relations. The scaling form for R is typical of instability phenomena. Numerical studies indeed show that small perturbations about spot solutions decay in time when $\eta > \eta_c$ but grow to form latent rings when $\eta < \eta_c$.

These results suggest the following mechanism of ring formation from small growing spots. A plant species characterized by a sufficiently large η , will deplete the soil-water density at the forefront of the growing spot to a level at which the spot can no longer expand, thus forming an asymptotic spot-like structure. In contrast, a small- η species,

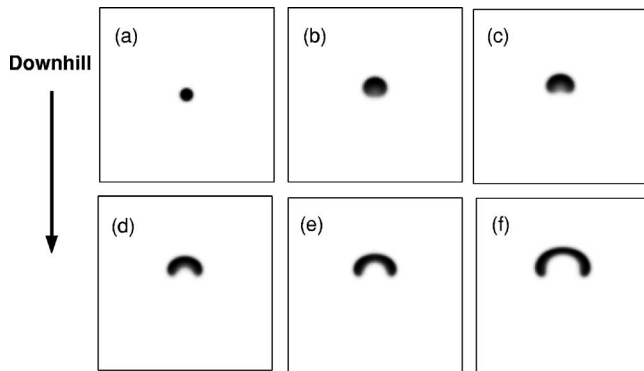


FIG. 11. Development of crescent patch forms on hill slopes. Snapshots of model simulations showing an initial spot evolving to form a crescent-like patch slowly migrating uphill. The times correspond to 2.5 yr (a), 15.5 yr (b), 22.5 yr (c), 30.5 yr (d), 37.5 yr (e), 49.5 yr (f). Parameters: $\eta=1.9$, slope= 2° and all other parameters are the same as in Fig. 8.

high current interest in ecology: facilitation by ecosystem engineers, species diversity along environmental gradients, and desertification. 393 394 395

A. Facilitation by ecosystem engineers 396

Plants are strongly affected by their physical (abiotic) environments, which determine the availability of crucial resources such as water, nutrients, and light. Plants also modify their abiotic environments, e.g., by soil-water uptake, nutrient consumption, shading of sunlight, or by changing infiltration rates. Some plant species, however, have more pronounced and significant effects on their abiotic environments than others. These species deserve special attention because of their potential ability to facilitate the growth of other species and thereby change species composition and richness. Species of this kind are often called “ecosystem engineers.”²⁸⁻³¹ 397 398 399 400 401 402 403 404 405 406 407 408

In the context of dryland vegetation, ecosystem engineering is realized by the ability of woody plant species, such as certain shrubs, to concentrate the water resource in the vegetation patches they form. The significantly higher soil-water densities in these patches as compared with the density in the surrounding bare soil provide habitats for herbaceous species that cannot tolerate the water stress in bare soil. 409 410 411 412 413 414 415 416

The results shown in Fig. 4 point towards a plant trait that strongly affects the engineering capacity: the root-system augmentation in response to biomass growth, quantified by η . Plant species with smaller η concentrate more water and therefore are better ecosystem engineers. Figure 6 shows that a given ecosystem engineer may lose its engineering capacity when the precipitation rate p is increased, and Fig. 5 shows that the engineering capacity can be lost as a result of crust disturbances which increase the infiltration rate in bare soil (by increasing f). 417 418 419 420 421 422 423 424 425 426

All these factors, controlled by η, p, f , affect ecosystem engineering by changing the relative strengths of the infiltration and uptake processes. Dominance of the former favors water concentration and positive engineering whereas dominance of the latter favors water depletion and negative engineering.³² Larger η values increase the water uptake process by extending the root system and therefore leads to negative engineering. Higher precipitation rates, p , significantly increase the patch size and therefore the number of individuals taking up water. The infiltration rate, on the other hand, increases only slightly, despite the increase of the biomass density, because of the weak biomass dependence of the infiltration rate at high biomass densities (see Fig. 1). As a result, increasing p tilts the water balance towards water uptake and negative engineering. Finally, higher f values increase the infiltration rate in bare soil and consequently reduce the flow of surface water into engineer’s patches. As a result, the amount of surface water infiltrating into the soil within a patch decreases, which tilts the water balance towards negative engineering. 427 428 429 430 431 432 433 434 435 436 437 438 439 440 441 442 443 444 445 446

Crossovers from negative to positive engineering, or from competitive to facilitative interactions, in woody-herbaceous systems have recently been observed in field studies along rainfall gradients.^{33,34} 447 448 449 450

368 needed for its further expansion. As Fig. 10 demonstrates, a 369 transition from rings to spots does occur by decreasing \bar{p} . 370 Increasing the parameter f has a similar effect; higher f val- 371 ues imply higher infiltration rates in bare soil and lesser 372 amounts of surface water accumulating at the vegetation 373 spot. The instability threshold, η_c , therefore depends on \bar{p} , f 374 and other parameters affecting the level of soil-water at the 375 forefront of a vegetation spot.

376 The studies described so far apply to plane topography 377 ($\nabla\zeta=0$). On a slope spots destabilize to crescent-like patches 378 migrating uphill as Fig. 11 shows. The uphill part of the spot 379 receives runoff generated by the large bare area uphill, while 380 the downhill part receives a small amount of that runoff and 381 loses runoff downhill. As a result the spot expands in the 382 uphill direction and retreats in the downhill direction, form- 383 ing a crescent patch form. Figure 12 shows a crescent patch 384 form of *Asphodelus ramosus* on a slope observed in the 385 northern Negev.

386 VI. ECOLOGICAL IMPLICATIONS

387 The studies of localized structures described in the pre- 388 vious sections have significant ecological implications in 389 terms of habitat creation, by redistribution of the water re- 390 source, and in terms of resilience to environmental changes 391 and disturbances, such as droughts and grazing. We briefly 392 discuss these implications in the context of three topics of



FIG. 12. A crescent-like patch of *Asphodelus ramosus* on a slope observed in the northern Negev (200 mm/yr). Typical patches are 20 cm long.

451 B. Species diversity along environmental gradients

452 The dominant plant life-forms in drylands are woody
453 and herbaceous vegetation. Because of water limitation typi-
454 cal landscapes are mosaics of woody patches and open non-
455 woody areas. Species diversity studies mostly focus on the
456 herbaceous life form that can reside both in the woody
457 patches and in the open areas, depending on the environmen-
458 tal conditions and the engineering capacity of the woody
459 species.

460 The results presented in Fig. 6 suggest that at high pre-
461 cipitation rates herbaceous species will mostly occupy the
462 open areas because the soil-water density there is higher than
463 in woody patches, and can be above the tolerance limit to
464 water stress. In contrast, at low precipitation rates herbaceous
465 species may not tolerate the water stress in the open areas
466 and will mostly reside in the mesic woody patches. This
467 implies that species richness may not necessarily decline
468 along the rainfall gradient, but species composition is ex-
469 pected to change because of the different environments
470 woody patches and open areas provide. Shading-sensitive
471 herbaceous species that occupy the open areas in high rain-
472 fall regions may disappear in low rainfall regions because the
473 only areas that are mesic enough are the woody patches
474 which block sunlight. In contrast, grazing-sensitive species
475 that cannot tolerate the grazing stress in the open areas of
476 high rainfall regions can colonize the woody patches in low
477 rainfall regions because of the protection they provide. A
478 recent study of a two-species version of the model equations,
479 describing a woody-herbaceous system, confirms these
480 expectations.³⁵

481 The results presented in Fig. 5 suggest that gradients of
482 soil conditions resulting in different infiltration rates can also
483 affect species richness and/or composition. Regions sub-
484 jected to grazing activity, for example, will suffer from bro-
485 ken soil-crust and consequently will experience higher infil-
486 tration rates (higher f values) in the open areas. While woody
487 patches in undisturbed regions may show ring-like water dis-
488 tributions (Fig. 5, $f=0.04$), patches in moderately disturbed
489 regions (Fig. 5, $f=0.12$) can show spot-like distributions.
490 Thus, shading-sensitive species that cannot grow under the
491 woody canopies in moderately disturbed regions, may appear
492 at the peripheries of woody patches in undisturbed regions,
493 where the soil-water density reaches its maximal value. In
494 contrast, grazing-sensitive species that can grow under the
495 woody canopies in moderately disturbed regions, may not be
496 able to grow in undisturbed regions. Patches in highly dis-
497 turbed regions (Fig. 5, $f=0.48$) may show no water concen-
498 tration, and herbaceous vegetation may not grow at all.

499 The formation of biomass ring structures may have ad-
500 ditional effects on species composition and richness, but we
501 are not aware of empirical studies addressing this question.

502 C. Desertification

503 Desertification is defined as an irreversible decrease in
504 biological productivity induced by an environmental change,
505 and is captured by the model in bistability ranges of bare-soil
506 and vegetation-pattern states, which are also the ranges
507 where localized structures appear. One scenario of a deserti-

508 fication process is illustrated in Fig. 2.⁵ A precipitation down-
509 shift to values below the threshold p_0 can induce a transition
510 from the spot-pattern state, \mathcal{S} , to the bare-soil state, \mathcal{B} , be-
511 cause the former no longer exists at these precipitation val-
512 ues (see arrow in Fig. 2). The transition is irreversible be-
513 cause the bare-soil state remains stable even when the
514 precipitation rate resumes its original value. Transitions of
515 this kind are often referred to as “catastrophic regime
516 shifts.”^{14,36} The same scenario represents desertification due
517 to overgrazing, for grazing in the model is captured by the
518 biomass-loss rate, M , which is inversely proportional to the
519 dimensionless precipitation parameter p (see Table I).

520 Another scenario of desertification is illustrated in Fig. 5
521 with a species having low tolerance to water stress ($\eta=2$). A
522 crust-removal disturbance that increases f beyond the thresh-
523 old f_c results in a transition to the bare-soil state (because of
524 the increased infiltration in bare soil and the corresponding
525 decrease in surface water accumulating at the vegetation
526 patch). The transition is irreversible because the bare-soil
527 state remains stable even when the crust recovers.

528 VII. CONCLUSION

529 The model Eqs. (1)–(4) and their extension to multispec-
530 ies plant communities³⁵ provide a theoretical platform for
531 studying a variety of problems related to the patchiness, re-
532 siliance, and diversity of dryland vegetation. A few such
533 problems have been addressed in this paper, including (i)
534 biomass-water relationships in spot-like vegetation patches,
535 (ii) formation mechanisms of ringlike and crescent-like veg-
536 etation patches, (iii) resilience of vegetation patches to dis-
537 turbances and precipitation downshifts, (iv) conditions for
538 ecosystem engineering by plants, and (v) transitions from
539 negative to positive engineering along environmental gradi-
540 ents and the implications to species-diversity change.

541 The results of these studies are consistent with field ob-
542 servations of transitions from competition to facilitation in
543 woody-herbaceous systems along rainfall gradients,^{33,34} with
544 field observations of spot, ring, and crescent-like patches,
545 and with the observation that rings in nature are formed by
546 dense clonal plants. Theoretical results obtained with the
547 same model equations for extended vegetation states^{9–11} are
548 also consistent with available field observations.^{13–15} How-
549 ever, careful attempts to test theoretical predictions in con-
550 trolled laboratory experiments are still scarce.¹⁸ In particular,
551 more effort is needed to resolve the soil-water distributions
552 in vegetation patches, and to study their relations to the
553 aboveground biomass distributions as the patches evolve in
554 time, and under different environmental conditions.¹⁷

555 ACKNOWLEDGMENTS

556 We thank M. Shachak, A. Novoplansky, E. Sheffer, Y.
557 Seligmann, J. von Hardenberg, and A. Provenzale for helpful
558 discussions. This study has been supported by the James S.
559 McDonnell Foundation and by the Center for Complexity
560 Science.

¹Drylands are water-limited systems comprising about 40% of the terres-
561 trial earth surface.

²R. Lefever and O. Lejeune, Bull. Math. Biol. 59, 263 (1997). 563

- 564 ³O. Lejeune and M. Tlidi, *J. Veg. Sci.* **10**, 201 (1999). 596
- 565 ⁴C. Klausmeier, *Science* **284**, 1826 (1999). 597AQ:
- 566 ⁵J. von Hardenberg, E. Meron, M. Shachak, and Y. Zarmi, *Phys. Rev. Lett.* 598 #2
- 567 **87**, 198101 (2001). 599
- 568 ⁶T. Okayasu and Y. Aizawa, *Prog. Theor. Phys.* **106**, 705 (2001). 600
- 569 ⁷M. Rietkerk *et al.*, *Am. Nat.* **160**, 524 (2002). 601
- 570 ⁸E. Meron, E. Gilad, J. von Hardenberg, M. Shachak, and Y. Zarmi, *Chaos, Solitons Fractals* **19**, 367 (2004). 602
- 571 ⁹E. Gilad, J. von Hardenberg, A. Provenzale, M. Shachak, and E. Meron, *Phys. Rev. Lett.* **93**, 981051 (2004). 603
- 572 ¹⁰H. Yizhaq, E. Gilad, and E. Meron, *Physica A* **356**, 139 (2005). 604
- 573 ¹¹E. Gilad, J. von Hardenberg, A. Provenzale, M. Shachak, and E. Meron, *J. Theor. Biol.* **244**, 680 (2007). 605
- 574 ¹²M. Cross and P. Hohenberg, *Rev. Mod. Phys.* **65**, 851 (1993). 606
- 575 ¹³C. Valentin, J. d'Herbès, and J. Poesen, *Catalysis* **37**, 1 (1999). 607
- 576 ¹⁴M. Rietkerk, S. Dekker, P. de Ruiter, and J. van de Koppel, *Science* **305**, 1926 (2004). 608
- 577 ¹⁵N. Barbier, P. Coutron, J. Lejoly, V. Deblauwe, and O. Lejeune, *J. Ecol.* 609
- 578 **94**, 537 (2006). 610AQ:
- 579 ¹⁶Various factors contribute to this effect, including biological crusts that 611 #3
- 580 grow on bare soil and reduce the infiltration rate, but do not develop in 612
- 581 vegetation patches due to shading and litter formation, and soil mounds, 613
- 582 formed by litter accumulation and dust deposition, that intercept runoff. 614
- 583 ¹⁷F. Ludwig, H. de Kroon, F. Berendse, and H. Prins, *Ecology* **170**, 93 615
- 584 (2004). 616
- 585 ¹⁸E. Sheffer, H. Yizhaq, E. Gilad, M. Shachak, and E. Meron (submitted). 617
- 586 ¹⁹We chose in this paper to view the closely related water-uptake and root- 618
- 587 augmentation processes as two distinct feedbacks, one negative and one 619
- 588 positive, rather than lumping them together under a single name, "uptake 620
- 589 feedback," as we did in earlier publications (Refs. 9 and 11). 621
- 590 ²⁰B. Walker, D. Ludwig, C. Holling, and R. Peterman, *J. Ecol.* **69**, 473 622AQ:
- 591 (1981). 623 #4
- 592 624
- 593
- 594
- 595
- 596
- 597
- 598
- 599
- 600
- 601
- 602
- 603
- 604
- 605
- 606
- 607
- 608
- 609
- 610
- 611
- 612
- 613
- 614
- 615
- 616
- 617
- 618
- 619
- 620
- 621
- 622
- 623
- 624
- ²¹S. Campbell, J. Seeler, and S. Glolubic, *Arid Soil Res. Rehab.* **3**, 217 (1989). 596
- ²²The bifurcation is subcritical (supercritical) depending on whether the quantity $2\eta\nu/[\nu(1-\rho)+\gamma]$ is greater (lower) than unity. 597AQ:
- ²³O. Lejeune, M. Tlidi, and P. Coutron, *Phys. Rev. E* **66**, 010901 (2002). 598 #2
- ²⁴F. Vasek, *Am. J. Bot.* **67**, 246 (1980). 599
- ²⁵E. White, *Rangelands* **11**, 154 (1989). 600
- ²⁶S. Wikberg and L. Mucina, *J. Veg. Sci.* **13**, 677 (2002). 601
- ²⁷L. Lovett Doust, *J. Ecol.* **69**, 743 (1981). 602
- ²⁸C. Jones, J. Lawton, and M. Shachak, *Oikos* **69**, 373 (1994). 603
- ²⁹C. Jones, J. Lawton, and M. Shachak, *Ecology* **78**, 1946 (1997). 604
- ³⁰K. Cuddington, J. Byers, A. Hastings, and W. Wilson, *Ecosystem Engineers: Concepts, Theory, and Applications in Ecology* (Academic, New York) (in press). 605
- ³¹Ecosystem engineers need not necessarily be plant species. They can be micro-organisms such as cyanobacteria in drylands which reduce the infiltration rate of surface water by forming soil crusts, thereby increasing the flow of surface water into lower places. Ecosystem engineers can also be animals. A well known example is the North American beaver which forms small ponds by building dams across rivers. 606
- ³²Positive (negative) engineering refers to situations in which the maximal soil-water density in the engineer's patch is higher (lower) than the soil-water density in bare soil. 607
- ³³F. Pugnaire and M. Luque, *Oikos* **93**, 42 (2001). 608
- ³⁴C. Holzapfel, K. Tielbörger, H. Paragb, J. Kigel, and M. Sternberg, *J. Appl. Ecol.* **7**, 268 (2006). 609
- ³⁵E. Gilad, M. Shachak, and E. Meron (unpublished). 610
- ³⁶M. Scheffer, S. Carpenter, J. Foley, C. Folke, and B. Walker, *Nature* (London) **413**, 591 (2001). 611

AUTHOR QUERIES — 008793CHA

- #1 Author: See Ref. 18. Please include the article title or update
- #2 Author: Provide the whole title and coden for Refs. 21, 25
- #3 Author: Update Ref. 30
- #4 Author: Provide the article title or update Ref. 35
- #5 Author: For Figures 7 and 8: Is Ref. 18 published yet. If the copyright has already been transferred, the copyright holder has to be acknowledged for publication of this article.

PROOF COPY 008793CHA